HHS Public Access

Author manuscript

Acc Chem Res. Author manuscript; available in PMC 2024 September 15.

Published in final edited form as:

Acc Chem Res. 2023 June 20; 56(12): 1578–1590. doi:10.1021/acs.accounts.3c00151.

Ligand Chemistry in Anti-tumor Theranostic Nanoparticles

Guanyou Lin, **Miqin Zhang***

Department of Materials Science and Engineering, University of Washington, Seattle, Washington 98195, United States

Conspectus

Theranostic nanoparticles' potential in tumor treatment has been widely acknowledged thanks to their capability of integrating multifaceted functionalities into a single nanosystem. Theranostic nanoparticles are typically equipped with an inorganic core with exploitable physical properties for imaging and therapeutic functions, bioinert coating for improved biocompatibility and immunological stealth, controlled drug loading-release modules and ability to recognize specific cell type for uptake. Integrating multiple functionalities in a single nanosized construct requires sophisticated molecular design and precise execution of assembling procedures. Underlying the multifunctionality of theranostic nanoparticles, ligand chemistry plays a decisive role in translating theoretical designs into fully functionalized theranostic nanoparticles. The ligand hierarchy in theranostic nanoparticles is usually threefold. As they serve to passivate nanoparticle's surface, capping ligands form the first layer directly interfacing with the crystalline lattice of inorganic core. The size and shape of nanoparticles are largely determined by the molecular property of capping ligands so that they have profound influences on nanoparticles' surface chemistry and physical properties. Capping ligands are mostly chemically inert, which necessitates the presence of additional ligands for drug loading and tumor targeting. The second layer is commonly utilized for drug loading. Therapeutic drugs can either be covalently conjugated onto the capping layer or non-covalently loaded onto nanoparticle via drug loading ligands. Drug loading ligands need to be equally versatile in properties to accommodate the diversity of drugs. Biodegradable moieties are often incorporated into drug loading ligands to enable smart drug release. With the aid of targeting ligands which usually stand the tallest from the nanoparticle surface to seek for and bind to its corresponding receptors on the target, theranostic nanoparticles can preferentially accumulate at tumor site to attain higher precision and quantity for drug delivery. In this account, properties and utilities of representative capping ligands, drug loading ligands and targeting ligands are reviewed. Since these types of ligands are often assembled in close vicinity to each other, it is essential for them to be chemically compatible and able to function in tandem with each other. Relevant conjugation strategies and critical factors posing significant impact on ligands' performance on nanoparticles are discussed. Representative theranostic nanoparticles are presented to showcase how different types of ligands function synergistically from a single nanosystem. Lastly, the technological outlook of evolving ligand chemistry on theranostic nanoparticles is provided.

*Corresponding Author Fax: (206) 543-3100. mzhang@uw.edu. Miqin Zhang.

Author Contributions

The manuscript was written through contributions of all authors. All authors have given approval to the final version of the manuscript.

The authors declare no competing financial interest.

Graphical Abstract

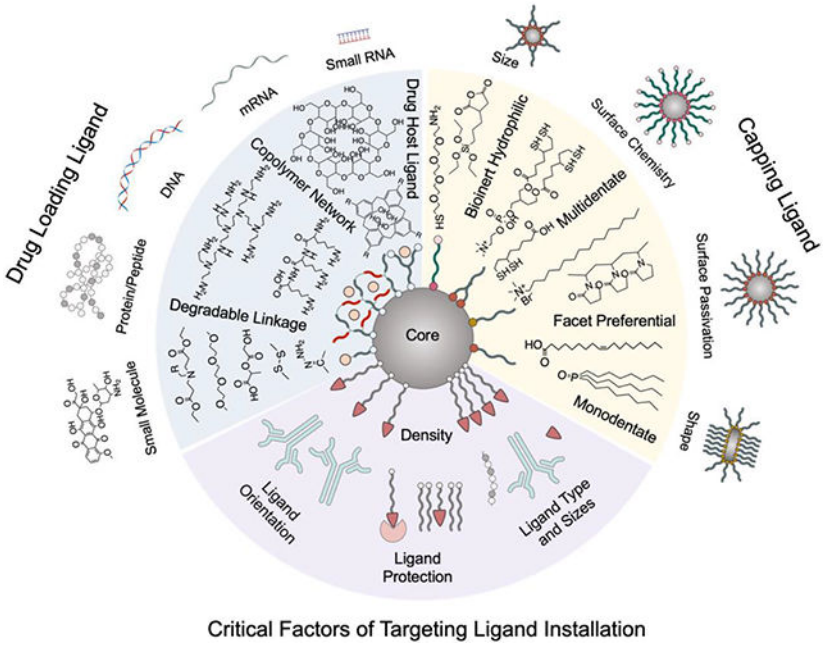

Critical Factors of Targeting Ligand Installation

1. Introduction

Nanoparticles bearing both therapeutic and diagnostic (theranostic) functions are indispensable in fulfilling the diverse needs in nanomedicine for tumor treatments. Many theranostic nanoparticles have a core and multiple layers usually including a capping layer, a drug loading layer and a targeting ligand layer. Ligand chemistry regulates the assembly of these layers on theranostic nanoparticles and determines their appearances, surface properties and functionalities. The inorganic crystalline cores confer nanoparticles with electromagnetic properties for biosensing, imaging and therapeutic purposes. Adjacent to the core lies a capping layer which forms a stabilizing layer on the inorganic core and thereby insulating the core from further growth or reaction. The capping ligand-core interface chemistry dictates nanoparticle's physicochemical properties critical to theranostic applications. Theranostic nanoparticles of 50-100 nm in size exhibited tremendous translational values in clinic settings.[4] Shape also significantly affects the biological utility of nanoparticles. Although spherical nanoparticles are stable and easily functionalized, anisotropic nanoparticles can exhibit better drug delivery potential due to their tumbling flow dynamics in bloodstream.[5] Since inorganic cores are usually not on the same size scale as drug molecules nor do they possess the structural pliability for drug molecules to situate themselves, drug loading ligands are needed to reliably provide shelters for drugs. Although the enhanced permeability and retention (EPR) effect can passively assist nanoparticle accumulation in tumors, the resultant bioavailability of nanoparticles at target sites remains suboptimal. As such, targeting ligands are often necessary to increase nanoparticles' accumulation at tumor sites. Surface conjugation chemistry plays an essential role in endowing nanoparticles with functional modules including drug-loading and targeting ligands to provide biocompatibility, capacity of loading multiple therapeutic agents

and spatiotemporal control over their pharmacokinetic profiles and reporter functions.[6] Thus, choosing a collection of ligands that are compatible in chemistry and can work in tandem with each other is essential in theranostic nanoparticle design.

In the following sections, different types of ligands, their influence on nanoparticle properties and performance, and important ligand conjugation chemistry will be discussed. Individual cases of recently developed theranostic nanoparticles will be analyzed to provide insights of incorporating different ligands into a single nanoparticle and the application of such nanoparticle.

2. Capping ligands

Capping ligands usually contain an anchoring group to bind with metallic cores, a spacer module and possible functional groups for future modification. The selection of capping ligands should be judiciously balanced between the following factors: the binding strength and orientation between capping ligands and core lattice, the available function groups present on the capped nanoparticle, the environment nanoparticles will be applied to. Pairing capping ligands with suitable cores while meeting these factors is challenging. Characterization techniques often fall short in providing comprehensive analysis of ligand-core interface on atomic scale due to its complexity. The understanding of ligand-core interfaces mostly relies on the rationalization based on the complementary pieces of information yielded by instruments. Stringent control of reaction conditions is then required while synthesizing capped nanoparticles because slight variations may result in defects which are undetectable by instruments but could profoundly influence the downstream applications of nanoparticles. Therefore, the synthesis procedure of capped nanoparticles should be kept as straightforward as possible for maneuverability, consistency and potential scaling up into large scale production.

2.1 The Anchoring Group of Capping Ligands

The binding between the ligand and inorganic core relies on the electron donation from the electronegative atoms in ligand's anchoring group to electrophilic undercoordinated metal ions. The anchoring groups of capping ligands often contain hydroxyl, carboxyl, thiol, phosphine and amine groups (Figure 1a).[7] The electronegative atoms in these functional groups (e.g. O, N, P, S) usually take the form of either a lone pair electron donor to coordinate with metal ions, or a singlet electron donor that shares a mutual pair of electrons with a metal ion to form a covalent bond.[8] Metal ions can be more electronegative than ligands on relatively rarer cases so that the ligand would serve as an electron acceptor. Therefore, atomic properties (e.g., atomic radius, oxidation state and polarizability) related to the electron donating and accepting between electronegative atoms and metal ions largely decide ligands' binding strength. Besides the atoms which directly interface with the metallic lattice, ligand's molecular structure also affects binding strength as other atoms in the ligand can impose steric hindrance and electronic distortions on metal-ligand bonds. Although ligands with high binding affinity or multiple anchoring groups (multidentate) can facilitate the formation of stable and small nanoparticles, these ligands will be difficult to remove via ligand exchange (Figure 1b). A good example of capping ligand is sodium

citrate which is used to cap metallic cores especially noble metals in aqueous solution. Once bound, the citrate ligand layer serves as a electrostatic repulsion layer to stabilize the core size.[9] Gold nanoparticles with tunable sizes ranging from 3.6 nm to 200 nm and iron oxide cores ranging from 4 to 20 nm have been successfully synthesized with sodium citrate as capping ligands.[10,11] The shortcoming of sodium citrate is that the binding affinity of citrate on noble metallic cores is relatively weak (6.7 kJ/mol on gold).[12] Another type of ligands commonly employed to cap noble metallic cores is thiolate ligand due to its high binding energy with metal surfaces (126-167 kJ/mol on gold).[13] Thiolate ligands have been frequently reported to participate in the synthesis of ultrasmall gold nanoparticles only a few nanometers in size.[14] Representative hydrophobic capping ligands such as trioctylphosphine oxide (TOPO), oleic acid and oleylamine also contain phosphine, carboxyl and amine in their headgroups for metal coordination. Due to the presence of long hydrocarbon tail, these ligands have the ability to coat inorganic cores of various compositions in organic solvents.[15,16]

2.2 Capping Ligands' Influence on Nanoparticle Shape

The choice of capping ligand can have profound effects on nanoparticle's shape. Ligands can preferentially bind to specific crystal facets with matching atomic packing density, structural symmetry and reaction energy to passivate those facets from further atomic growth.[17] Meanwhile, new atoms will continue to deposit onto crystal facets unbound by ligands and cause epitaxial growth. It is also important to consider the kinetics of supplied metal atoms and ligands in solutions. Metal atoms need to have sufficient energy and time to diffuse to and deposit at the optimal site on the pre-formed nucleus for growth. When metal atoms cannot reach the optimal deposition site either because the atoms do not have sufficient energy and time to travel such distance or because the sites are already passivated by capping ligands, they will settle for relatively unstable sites and yield thermodynamically less-favored anisotropic shapes. Therefore, the reaction temperature, real-time concentrations of metal precursor and capping ligands collectively control the size and shape of inorganic cores. There are some ligands that exhibit strong binding preference on certain crystal planes (Figure 1c). For example, amphiphilic cetyltrimethylammonium bromide (CTAB) favors binding to the more densely packed {100} gold facet than the {111} plane. Since the growth along the {100} plane is inhibited by CTAB, the {111} plane becomes the growing tip of a nanorod. It has also been found that longer CTAB tail leads to higher nanorod aspect ratio due to hydrophobic stabilization.[18] Another capping ligand with facet preferential binding is polyvinyl pyrrolidone (PVP) which has been found to assist the formation of Ag nanowire and Pt nanocube.[19] Since capping ligands do not unilaterally dictate nanoparticle's shape, spherical nanoparticles' capping ligands such as sodium citrate, TOPO and oleic acid have also participated in synthesizing nanoparticles with anisotropic shape including polygon, rod and cone.[9,20,21]

2.3 Capping Ligands' Influence on Nanoparticle Surface Properties

The main body of a capping ligand is the spacer module which can be hydrophobic or hydrophilic. Nanoparticles for biological applications are commonly coated with hydrophilic ligand layers. For inorganic nanoparticle cores capped with hydrophobic capping ligands in organic solvents, ligand exchange is needed to replace hydrophobic ligands with

hydrophilic ligands (Figure 1d). Depending on the kinetics of the incoming and the leaving ligands, ligand exchange can proceed through associative pathway, dissociative pathway or intermediate pathway in between.[22] For the associative pathway, incoming ligands bind to metal ions to form intermediate complex before original ligands leave, minimizing the energetic penalty incurred by breaking the bond between the strong-binding ligand and core.[23] However, metal ions often need to be undercoordinated and possess available sites for incoming ligands to bind before losing the original ligands. Alternatively in the dissociative pathway, especially for sterically crowded surface with high ligand packing density, the attachment of replacement ligands occurs after original ligands have desorbed from core.[8] Ligands with stronger binding affinity are typically needed to replace the weakly bound ligand. For example, the weakly bound citrate ligand on gold surface can be replaced by a phosphine ligand which can then be further replaced by the strongest-binding thiol ligand.[24]

Polyethylene glycol (PEG) and silanes are two essential spacer modules often integrated in the hydrophilic ligands for improving nanoparticle's colloidal stability and immunological stealth in biological milieu as they are both hydrophilic, chemically inert and biocompatible.[25,26] PEG is usually equipped with reactive groups such as amines, carboxyl or thiols for core anchoring and further functionalizations.[27] It is worth noting that excessive PEG can reduce nanoparticles' cell uptake efficiency so that the molecular weight of PEG and the surface density of PEG on nanoparticles need to be tuned for optimal cell entry.[26] Silane ligands crosslink with each other in aqueous condition to form a siloxane shell which serves as a robust protective layer on nanoparticle core. Similar to PEG, silane ligand molecules can also be functionalized with reactive groups so that the siloxane shell is open to further functionalization. Since capping ligands usually lack reactive sites to interact with other molecules, more ligands are needed to functionalize nanoparticles with drug loading and targeting utilities.

3. Drug loading ligands

Drugs can be drastically different in sizes, hydrophilicity and molecular structure and hence requires diverse delivery systems. Drugs are commonly loaded onto nanoparticle non-covalently for facile drug release. If a drug molecule possesses reactive groups that can be utilized for conjugation without affecting its therapeutic efficacy, it can be modified with biocompatible polymer and directly conjugated onto the inorganic core. Drug-nanoparticle conjugates have been reported to greatly suppress cancer cell's drug resistance as they can effectively bypass cancer cells' efflux pump.[28] The drug releasing profiles of nanoparticles are often tested in aqueous buffer at desired pH and temperature to mimic the physiological conditions in tumor microenvironment. Nonetheless, this approach, though convenient and can provide useful information, neglects the presence of serum proteins and the physical state of nanoparticles after crossing biological barriers. It is therefore critical to study nanoparticles' drug releasing performance in a more biologically relevant milieu such as that in cytoplasm. An overview of representative drug-loading strategies is illustrated in Figure 2.

3.1 Conjugating Drug Loading Ligands onto Capped Nanoparticle Core

Attachment of drug loading ligands onto inorganic cores often involves bioconjugation linking the functional groups such as amine, thiol, carboxyl on both capping ligands and drug loading ligands.[29] Since these functional groups do not readily react with each other, intermediator molecules which contain the reactive partners for these functional groups are needed to form the linkage. Succinimidyl ester, anhydride and epoxide are common reactive partners with amine groups to form amide bonds. Maleimide and iodoacetate are common reactive partners to form thioether bonds with thiol groups. Disulfides can go through disulfide exchange with thiols to form new disulfide bonds if one of the sulfurs in the original disulfide is linked to a stable leaving group. The conversion from amine to thiol group can be achieved by 2-iminothiolane (Traut's reagent) to avoid the nondirectional amine-amine crosslinking. Besides amine-thiol linkage, carbodiimide chemistry such as the 1-ethyl-3-(3-dimethylaminopropyl)carbodiimide (EDC) N-hydroxysuccinimide (NHS) chemistry is renowned for directly coupling amine with carboxyl groups. Heterobifunctional linkers (usually with PEG as spacer) equipped with reactive partners for different functional groups can reliably conjugate different ligands together.

Conventional bioconjugation chemistry relies on the reaction between functional moieties abundantly present on natural biomolecules and hence usually encounters the constraints of nonspecific crosslinking, off-targeted binding and perturbed biomolecular functions. Differently, functional groups participating in bioorthogonal chemistry are rarely found in natural biochemistry so that they can remain inert until meeting their reactive counterparts for chemoselective conjugation. Moreover, these functional groups can react rapidly even at low concentration, making them suitable for many biological experiments.[30] The most commonly used bioorthogonal chemistry is the cycloaddition between strained alkynes and azides. Derivatives of the smallest alkyne ring cyclooctyne showed promising 10^1 $M^{-1}S^{-1}$ kinetic rate when reacted with azides.[31] On the other hand, the discovery of the inverse-demand Diels-Alder reaction with the soaring kinetic rate of 10^5 $M^{-1}S^{-1}$ can complete tetrazine ligation on similar time and concentration scale as native biomolecular reaction, opening up possibilities of incorporating synthetic chemistry into biological environment.[32]

3.2 Drug Loading and Controlled Release Strategies

With its versatile modular designs, polymer molecule's properties can be subtly tuned by combining desirable monomer blocks to achieve precise control over drug loading and releasing utilities. Alternating sequence of hydrophilic and hydrophobic blocks can homogeneously distribute amphiphilicity across polymer chains whereas polymeric regions containing only hydrophobic blocks can create hydrophobic pockets to load hydrophobic drugs. The molecular structure of monomers is also critical. Branched polymers interact more strongly with therapeutics than linear polymers because their branching groups can coordinate therapeutic molecules to form stable complex. Polymeric regions with aromatic pendant groups can strongly bind with aromatic drugs via hydrophobic stacking.[33]

Monomer blocks in drug loading polymer usually serve one or multiple of three roles: drug binding, structural spacer and degradable linker. Drug binding monomers share matching properties in terms of polarity and shape symmetry with drug molecules.

Loading hydrophobic drugs commonly involves drug-host interaction with amphiphilic ligands. For example, the cone-shaped cyclodextrin, calixarenes and cucurbiturils have hydrophobic inner pockets for drug loading and hydrophilic outer surfaces for water solubility.[34] Hydrophobic drugs can also be rendered hydrophilic by chemically attached with biopolymers. A study has reported that hydrophobic drug doxorubicin (Dox) was chemically modified with PEG and PAMAM before attaching onto gold nanorods for photothermal-chemotherapy.[35] In another study, paclitaxel was directly conjugated onto amine-containing iron oxide nanoparticle surface to treat breast cancer.[36] On the other hand, hydrophilic therapeutics such as negatively charged nucleic acids would need polycations such as polyethyleneimine (PEI), polylysine (PLL) and poly(amidoamine) (PAMAM) for condensation before delivery.[37] Additional structural spacers such as PEG, poly(β-amino esters) (PBAE), poly(lactic-co-glycolic) acid (PLGA), and polysaccharides are sometimes integrated into polymers if the binding blocks exhibit undesired characteristics such as toxicity and hydrophobicity that need to be mitigated.[38] Degradable linkers confer drug delivery systems with controlled drug release mechanisms to improve the precision of drug release and promote the degradation and tissue clearance after drug release. Hydrolysable linkers such as PBAE and imines are highly popular in drug delivery as water is omnipresent in biological environment. It is crucial to tune hydrolysable linkers' degradation half-life to avoid premature or delayed drug release, respectively. Polymers with linkers capable of detecting the acidic tumor environment and intracellular redox species such as hydrazone, disulfide and β-carboxylic amide can have higher specificity in antitumor drug delivery.[39] There are also linkers susceptible to irradiation and magnetic field so that precise temporal control over drug release can be achieved. The ratio and sequence of drug binding blocks, structural spacers and degradable linkers need to be carefully designed and tested for optimal drug loading and release performance.

Notably, the presence of drug loading ligands can also dictate the nanoparticles' assembly state which has profound effect on nanoparticles' theranostic utilities. The principle lies in the conditional properties possessed by the ligands when subjected to varying environmental cues, of which pH-dependent charge switching and external stimuli (e.g., temperature, light, reactive oxygen species)-dependent structural change are mainly responsible.[40] For example, the imidazole group in a photodynamic drug chlorin e6 (ce6)-loaded ligand remains non-charged to promote nanoparticle assembly via hydrophobic interaction but becomes positively charged to break up the assembly in acidic tumor microenvironment[41] The otherwise self-quenched photodynamic therapeutic effect in the assembly state can be unleashed in the disassembly state for tumor killing. Similarly, clusters of iron oxide nanoparticles (IONP) assembled via acid labile hydrazone linkage can be disassembled into smaller individual IONP upon reaching the acidic tumor mass for deep tumor penetration and significantly enhanced T1 magnetic resonance contrast for tumor imaging [42] Alternative to relying on the drug-ligand interaction for drug loading and release, the controllable assembly state of nanoparticles provides more strategies for controlled release of theranostic utilities.

4. Targeting ligands

Tumor targeting can be either passive or active. Tumors can trap nanoparticles passively by their leaky vasculatures and poor lymphatic drainage, a phenomenon known as the enhanced permeability and retention (EPR) effect. However, the EPR effect varies significantly between different cancer types and is not reliable for precision therapy [43] Alternative to the EPR, active targeting strategies rely on the recognition of the overexpressed biomarkers on cancer cells by targeting ligands to facilitate nanoparticle's tumor extravasation, penetration and cellular uptake. It is a common approach to validate the biomarker overexpression by the target cells and compare the uptake of targeting ligands-conjugated nanoparticles by the target cells to that of bare nanoparticles in vitro. However, targeting ligand conjugation may alter the surface properties of nanoparticles and possibly change their cell uptake via mechanisms unrelated to the targeting ligand itself, especially when nanoparticles and cells are incubated in proximity in vitro. Therefore, nanoparticles' targeting efficiency should be reliably evaluated in vivo by measuring nanoparticles' bioavailability in tumors.

4.1 Popular Tumor Targeting Strategies

There are mainly two types of tumor-targeting ligands. One targets the cancer cells lurking deep in tumor tissue and the other targets the endothelial cells in tumor vasculature. Receptors commonly overexpressed by cancer cells include folate receptor, transferrin receptor, CD44 receptor and epidermal growth factor receptor (EGFR) because these receptors are responsible for the intake of fundamental nutrients and the activation of oncogenic proliferative pathway. Their corresponding ligands are folic acid, transferrin, hyaluronic acid and anti-EGFR monoclonal antibody (anti-EGFR mAb). Cancer cell-targeting nanoparticles equipped with these ligands can effectively recognize cancer cells but would lack the means to penetrate vasculature and extracellular matrix before reaching cancer cells, which precludes the interaction between nanoparticles and cancer cells. On the other hand, biomarkers commonly overexpressed by endothelial cells are vascular endothelial growth factors (VEGF), $\alpha v\beta 3$ integrin and vascular cell adhesion molecule-1 (VCAM-1) which are mainly responsible for forming new vasculatures and extracellular matrix in tumor. These biomarkers can be targeted by anti-VEGF mAb, derivatives of Arg–Gly–Asp (RGD) oligopeptides and anti-VCAM mAb. Single chain variable fragment (scFv) can be isolated from mAb to significantly reduce the size of targeting ligands while retaining original mAb's binding capability. Tumor vasculature-targeting nanoparticles can promote tumor extravasation via vasculature transcytosis, which is a dominant active intratumor transportation mechanism.[44] Nonetheless, these nanoparticles can fall short in effectively interacting with cancer cells for intracellular drug delivery. Alternatively, vasculature-targeting nanoparticles can pair with anti-angiogenic drugs to destroy vasculature and starve tumors to death, bypassing the need for direct confrontation with cancer cells.[45]

To be effective at both tumor extravasation and cancer cell uptake, some nanoparticles are equipped with transcytosis-targeting peptides and cancer cell targeting ligands to target both vasculature and cancer cells simultaneously.[46] Alternatively, there are also receptors overexpressed by both cancer cells and vasculature cells such as the glucose transporter (GLUT) receptor. Nanoparticles equipped with glucose as targeting ligand exhibited

improved performance in both vascular translocation and cancer cell uptake.[47,48] Notably, GLUT receptors have also been found to be highly and consistently expressed by endothelial cells in the blood brain barrier (BBB) which is a highly selective barrier commonly requiring receptor-mediated transcytosis to penetrate.[49] With glucose as targeting ligand, nanoparticles show enhanced accumulation in brain tissue for brain tumor treatments.[50] However, GLUT receptors are also highly expressed by other healthy cell types. Hence, a targeting ligand's utility in assisting penetration across multiple biological barriers may come with the compromise of reduced targeting specificity. Besides glucose, another promising BBB targeting ligand is chlorotoxin peptide as it also facilitates receptor-mediated transcytosis of nanoparticles.[51]

4.2 Critical Installation Factors of Targeting Ligands on Nanoparticles

Critical parameters of ligand installment on nanoparticles include ligand's density, orientation, and the curvature of nanoparticle's surface (Figure 3a, b). Insufficient targeting ligand installment diminishes nanoparticles' targeting capability. However, excessive installment could also have several adverse effects on cellular uptake.[52] First, the stealth of nanoparticle would be compromised as bioinert capping layer's exposure decreases. Second, high ligand density could deplete cellular receptors and block more nanoparticles from entering cells. Third, closely packed ligands could exert steric hindrance on each other and dampen ligand-receptor binding efficiency. Smaller nanoparticles enable higher ligand density as their high curvature helps ligands avoid each other. The molecular size of ligands poses restriction on feasible ligand density. The weak binding small molecule ligands can be installed onto nanoparticles at higher density to achieve sufficient receptor binding without increasing nanoparticle's size too much. One advantage for weak-binding small molecule ligand is that nanoparticles can be released easily after transcytosis across epithelial cells, facilitating tumor tissue penetration.[53] Large targeting ligands with high binding affinity only need to be installed at lower density to minimize size increase. Moreover, large biomolecules could have multiple reactive sites for conjugation so that the orientation of biomolecule on nanoparticle needs to be controlled for optimal targeting performance.

For better presentation, a spacer is often inserted between nanoparticle surface and targeting ligands so that targeting ligands can reach farther out to interact with their corresponding receptors. Ligands with longer spacer might cause heterogeneous ligand density on nanoparticle because they need more space to accommodate for their dynamic motion and shape.[54] Nonetheless, premature exposure of ligands prior to contact with their receptors risks off-target effect, unwanted immunorecognition and damages to the ligands. Ligand protection techniques have been explored to circumvent this issue (Figure 3c).[53,55] Ligands can be shielded by materials during transportation. Upon reaching target sites, these shielding materials can then be removed by environmental cues such as pH changes and overexpressed enzymes in tumor environment to reveal the ligand for receptor binding.[56,57] Furthermore, linkers capable of conformational change at acidic tumor environment have also been developed.[58,59] These linkers which are neutral and retracted at physiological pH can be protonated at low pH and extend themselves by charge repulsion to present the anchored targeting ligands.

5. Case Studies of Ligand Functionalized Multifunctional Nanoparticles

Different types of ligands have been discussed separately in earlier sections. These types of ligands function collectively as a system in a theranostic nanoparticle. Several representative examples of ligand-functionalized theranostic nanoparticles are presented in this section to illustrate various ligand integration strategies for treating different cancer types.

5.1 BBB-Targeting Delivery of Genetic Therapeutics for Brain Cancer Treatment

O6-methylguanine-DNA methyltransferase (MGMT) gene is responsible for chemotherapeutic resistance against temozolomide (TMZ) in brain tumor treatment. Chitosan-PEG-PEI (CP-PEI) copolymer was conjugated onto spherical 8 nm iron oxide nanoparticle (IONP) cores coated with siloxane shell and amine-PEG (PEG-NH_2) ligands (denoted as IONP-PEG-NH_2) to deliver siRNA (siMGMT) to silence MGMT gene.[1] The high molecular weight branched PEI (MW 25 kDa) was applied to effectively load siMGMT. Chitosan and PEG serve as the biocompatible structural blocks in the copolymer to mitigate the cytotoxicity of PEI. CP-PEI was synthesized first and then grafted on IONP-PEG-NH2 via bioconjugation chemistry (Figure 4a). IONP-CP-PEI-CTX was then loaded with siMGMT electrostatically to form the fully functionalized IONP-siMGMT-CTX which was 61 nm in size. In vivo biodistribution data demonstrated that IONP-siMGMT-CTX had high brain tissue accumulation which could later be effectively cleared out from healthy organs (Figure 4b). Notably, IONP-siMGMT-CTX was able to effectively suppress the MGMT expression in glioblastoma in vivo (Figure 4c). Therefore, co-administration of IONP-siMGMT-CTX and TMZ was able to halt glioblastoma's growth as confirmed by both MRI and survival data (Figure 4d-f). The targeted delivery of chemo-sensitizing genetic drugs by MRI imageable nanoparticles could greatly enhance the therapeutic efficacy of standardly used chemo drugs in clinic.

5.2 Targeted Delivery of Combinatorial Chemo-Immunotherapeutics for TNBC Treatment

To treat triple negative breast cancer (TNBC), an IONP-PEG-NH_2-based nanoparticle was developed to simultaneously deliver chemotherapeutic doxorubicin (Dox) and immunomodulatory polyinosinic:polycytidylic acid (Poly IC) to treat TNBC tumor.[2] Since the siloxane layer of IONP-PEG-NH_2 carries negative charges, the positively charged Dox can be deposited onto IONP-PEG-NH_2. Poly IC is intrinsically anionic and can be further deposited onto the cationic Dox layer to form a layer-by-layer assembly. Endoglin-binding peptide (EBP) was employed as the TNBC vasculature-targeting ligand. Heterobifimctional succinimidyl -PEG-maleimide (NHS-PEG-Mal) linker was used to lift EBP away from the therapeutic deposition layers (Figure 5a). The resultant IONP-Dox-Poly IC-EBP nanoparticle is 53 nm in size with surface potential of −17.8 mV. MRI and fluorescent imaging results both validate the tumor accumulation of IONP-Dox-Poly IC-EBP (Figure 5b-d). Most importantly, IONP-Dox-Poly IC-EBP induced severe apoptosis in tumor tissue which translates to significant tumor growth inhibition and better animal survival rate (Figure 5e, f). TNBC has been a notoriously difficult-to-treat type of tumor mostly because TNBCs cells do not express the typical biomarkers for breast cancer targeting. Therefore, the vasculature-targeting strategy would be a sound alternative for these "stealth" cancer cells.

5.3 Switchable Double-Gated Ligand Design for Spatiotemporal Drug Release Control

In another study, iron oxide was combined with a chitosan-coated mesoporous carbon dot to form dual-layered nanoshell for switchable chemotherapeutic drug release.[3] A mesoporous silica nanoparticle of 78 nm in diameter was used as the template to grow an iron oxide carbon dot shell. The silica core was then dissolved in ammonia water to create cavity for drug loading. Dox can be loaded into the central cavity by passing through the porous carbon shell and stabilized by carboxyl-Dox drug-host interaction and hydrogen bonding. Chitosan was then covalently conjugated onto the nanoshell surface to seal Dox in the pores and form chitosan-Dox-HMMC-NC (Figure 6a). Besides the covalent linkage, chitosan also binds to the carbon shell via hydrogen bonding and electrostatic adsorption. The main feature of chitosan-Dox-HMMC-NC is that the release of drug can be switched between “on” and “off” states by applying alternating magnetic field to vibrate the magnetite nanoparticle and produce heat. The drug host interaction and chitosan adsorption would then be weakened to open the “gates” to release Dox molecules (Figure 6b). Without alternative magnetic field to sustain the elevated temperature, chitosan would be re-adsorbed onto the nanoshell and the lesser energetic Dox would be stabilized in the cavity again. Notably, chitosan-Dox-HMMC-NC was able to achieve potent therapeutic synergy between chemotherapeutic and magnetic-induced hyperthermia both in vitro (Figure 6c) and in vivo (Figure 6d-e). This double gated switchable drug release mechanism highlights the advanced spatiotemporal control on molecular scale achievable by ligands.

5.4 Integration of Multiple Targeting, Drug Release and Therapeutic Modalities into A Single Nanosystem

To achieve multi-faceted targeting and therapeutic effects against breast cancer, a gold nanorod (GNR) was equipped with dual targeting ligands (HA and anti-HER2 antibody), dual therapeutic mechanisms (photosensitizer 5-aminolevulinic acid (ALA) and photothermal GNR) and Cy7.5 reporter (Figure 7a).[60] The final nanoparticle product GNR-HA-ALA/Cy7.5-HER2 is 55 nm in length and 14 nm in width. In the acidic tumor environment, high intracellular concentration of glutathione and hyaluronidase (HAase) collectively degrade the HA network and efficiently release Cy7.5, ALA and GNR in cytoplasm for imaging, photodynamic and photothermal therapeutic purposes (Figure 7b). When administered intravenously in vivo, GNR-HA-ALA/Cy7.5-HER2 was able to preferentially accumulate in breast tumors (Figure 7c). When the tumor site was exposed under near-infrared irradiation, the tumors on GNR-HA-ALA/Cy7.5-HER2 treated mice were effectively eliminated (Figure 7d, e). The multifaceted targeting, drug release and therapeutic modalities integrated in a single GNR-HA-ALA/Cy7.5-HER2 system demonstrate the diverse utilities ligand chemistry can endow to a theranostic nanoparticle.

6. Conclusion and Outlook

Theranostic nanoparticles have demonstrated promising research results on animal studies; but their clinical translation remains sluggish. The main challenge is low nanoparticle bioavailability at tumor sites. The majority of nanoparticles coated with bioinert layers can still be recognized as foreign materials by immune cells for sequestration, decimating nanoparticle’s chance to even travel anywhere near tumors. The EPR effect has been

shown to be responsible for the accumulation of only around 0.7% of total administered nanoparticles.[61] Biomarker's overexpression amount can be too minimal for nanoparticles to differentiate tumor cells from healthy cells. Furthermore, tumor's extracellular matrix and tumor associated macrophages sequester the majority of the nanoparticles arrived in tumor, leaving only less than 20 out of 1 million administered nanoparticles actually interacting with cancer cells.[62] Nanoparticles' stealth and targeting efficiency need to be significantly improved for clinical application. A possible solution to simultaneously enhances nanoparticles' immunological stealth and tumor homing efficiency is the novel cell membrane cloaking technology. Specifically, cell membranes from red blood cells (RBC), leukocytes or cancer cells can be physically cloaked onto nanoparticle.[63] Depending on the cloak type, the nanoparticle surface can inherit RBC's CD47 "don't eat me signal", and have immune cell's immunorecognition receptors and cancer cell's homologous targeting effects.[64]

Another obstacle in nanoparticle's clinical translation is the obsessiveness of developing a one-fits-all nanoparticle. This strategy is often unfitting as the disease states of patients can be too heterogeneous for any one type of nanoparticle to accommodate. Engineering nanoparticles with multi-faceted targeting and therapeutic modalities to treat a subgroup of patients with high precision and potency is more realistic.[65] The technology of Janus nanoparticles could help integrate more functionalities into a single nanoparticle by compartmentalizing the limited space of a nanoparticle. For example, Janus nanoparticles containing iron oxide-gold hybrid cores have been developed to harness both superparamagnetic and plasmonic properties for imaging and therapeutic applications.[66] Gold and iron oxide hemispheres can each be functionalized with different ligands to achieve asymmetric property distribution on the same nanoparticle. As nanoparticles become more complex, ligand chemistry would play an even more significant role in organizing their structures and functions. It is imperative to look beyond the mere appearances of nanoparticles and seek comprehensive understanding of the selection, the arrangement and the chemistry of ligands that build nanoparticles bottom-up.

Funding

This work was partially supported by National Institutes of Health Grant (NIH/NIBIB R01EB026890). M. Z. acknowledges the support of Kyocera Chair Professor Endowment.

Biographies

Guanyou Lin earned his B.S. in bioengineering from the University of Washington. He is currently pursuing his Ph.D. degree in materials science and engineering at the University of Washington. His current research interest is in synthesis and application of nanoparticle systems for gene delivery and combinatorial antitumor therapies.

Miqin Zhang is Kyocera Chair Professor of Materials Science in the Department of Materials Science and Engineering and Professor of Neurological Surgery at the University of Washington. She received her Ph.D. in 1999 from the University of California at Berkeley. Her research focuses on nanomaterials for cancer diagnosis and treatment,

biodegradable scaffolds for tissue engineering, and biosensors for detection of chemical and biological agents.

References

(1). Wang K; Kievit FM; Chiarelli PA; Stephen ZR; Lin G; Silber JR; Ellenbogen RG; Zhang M; Wang K; Stephen ZR; Lin G; Zhang M; Kievit FM; Chiarelli PA; Silber JR; Ellenbogen RG SiRNA Nanoparticle Suppresses Drug-Resistant Gene and Prolongs Survival in an Orthotopic Glioblastoma Xenograft Mouse Model. Advanced Functional Materials 2021, 31 (6), 2007166. 10.1002/ADFM.202007166. [PubMed: 33708035] Iron oxide-mediated blood brain barrier-targeting delivery of genetic therapeutics to knockdown glioblastoma's chemoresistance.

(2). Mu Q; Lin G; Jeon M; Wang H; Chang FC; Revia RA; Yu J; Zhang M Iron Oxide Nanoparticle Targeted Chemo-Immunotherapy for Triple Negative Breast Cancer. Materials Today 2021, 50, 149–169. 10.1016/J.MATTOD.2021.08.002. [PubMed: 34987308] Iron oxide nanoparticles co-deliver chemo and immunotherapeutic drugs for triple negative breast tumor treatment.

(3). Wang H; Mu Q; Revia R; Wang K; Zhou X; Pauzauskie PJ; Zhou S; Zhang M Chitosan-Gated Magnetic-Responsive Nanocarrier for Dual-Modal Optical Imaging, Switchable Drug Release, and Synergistic Therapy. Advanced Healthcare Materials 2017, 6 (6), 1601080. 10.1002/adhm.201601080. Switchable double-gated controlled drug release system.

(4). Albanese A; Tang PS; Chan WCW The Effect of Nanoparticle Size, Shape, and Surface Chemistry on Biological Systems. Annual Review of Biomedical Engineering 2012,14 (1), 1–16. 10.1146/annurev-bioeng-071811-150124.

(5). Blanco E; Shen H; Ferrari M Principles of Nanoparticle Design for Overcoming Biological Barriers to Drug Delivery. Nature Biotechnology 2015, 33 (9), 941–951. 10.1038/nbt.3330.

(6). Lin G; Revia RA; Zhang M Inorganic Nanomaterial-Mediated Gene Therapy in Combination with Other Antitumor Treatment Modalities. Advanced Functional Materials. Wiley-VCH Verlag January 2021, p 2007096. 10.1002/adfm.202007096.

(7). Heuer-Jungemann A; Feliu N; Bakaimi I; Hamaly M; Alkilany A; Chakraborty I; Masood A; Casula MF; Kostopoulou A; Oh E; Susumu K; Stewart MH; Medintz IL; Stratakis E; Parak WJ; Kanaras AG; lbj UK The Role of Ligands in the Chemical Synthesis and Applications of Inorganic Nanoparticles. 2019. 10.1021/acs.chemrev.8b00733.

(8). Boles MA; Ling D; Hyeon T; Talapin DV The Surface Science of Nanocrystals. Nature Materials 2016 15:2 2016,15 (2), 141–153. 10.1038/nmat4526.

(9). Patungwasa W; Hodak JH PH Tunable Morphology of the Gold Nanoparticles Produced by Citrate Reduction. Materials Chemistry and Physics 2008,108 (1), 45–54. 10.1016/J.MATCHEMPHYS.2007.09.001.

(10). Bastús NG; Comenge J; Puntes V Kinetically Controlled Seeded Growth Synthesis of Citrate-Stabilized Gold Nanoparticles of up to 200 Nm: Size Focusing versus Ostwald Ripening. Langmuir 2011, 27 (17), 11098–11105. 10.1021/LA201938U/SUPPL_FILE/LA201938U_SI_001.PDF. [PubMed: 21728302]

(11). Laurent S; Forge D; Port M; Roch A; Robic C; Vander Elst L; Muller RN Magnetic Iron Oxide Nanoparticles: Synthesis, Stabilization, Vectorization, Physicochemical Characterizations and Biological Applications. Chemical Reviews 2008, 108 (6), 2064–2110. 10.1021/CR068445E/ASSET/IMAGES/CR-2006-08445E_M042.GIF. [PubMed: 18543879]

(12). Dinkel R; Braunschweig m; Peukert W. Fast and Slow Ligand Exchange at the Surface of Colloidal Gold Nanoparticles. 2015. 10.1021/acs.jpcc.5b11055.

(13). Nuzzo RG; Dubois LH; Allara DL Fundamental Studies of Microscopic Wetting on Organic Surfaces. 1. Formation and Structural Characterization of a Self-Consistent Series of Polyfunctional Organic Monolayers. Journal of the American Chemical Society 1990, 112 (2), 558–569. 10.1021/JA00158A012/ASSET/JA00158A012.FP.PNG_V03.

(14). Lohse SE; Dahl JA; Hutchison JE Direct Synthesis of Large Water-Soluble Functionalized Gold Nanoparticles Using Bunte Salts as Ligand Precursors. Langmuir 2010, 26 (10), 7504–7511. 10.1021/LA904306A/SUPPL_FILE/LA904306A_SI_001.PDF. [PubMed: 20180591]

(15). Niezgoda JS; Harrison MA; Mcbride JR; Rosenthal SJ Novel Synthesis of Chalcopyrite Cu x In y S 2 Quantum Dots with Tunable Localized Surface Plasmon Resonances. 2012. 10.1021/cm3021462.

(16). Liu X; Wang X; Zhou B; Law WC; Cartwright AN; Swihart MT Size-Controlled Synthesis of Cu2-XE (E = S, Se) Nanocrystals with Strong Tunable near-infrared Localized Surface Plasmon Resonance and High Conductivity in Thin Films. Advanced Functional Materials 2013, 23 (10), 1256–1264. 10.1002/ADFM.201202061.

(17). Xia Y; Xia X; Peng HC Shape-Controlled Synthesis of Colloidal Metal Nanocrystals: Thermodynamic versus Kinetic Products. Journal of the American Chemical Society 2015,137 (25), 7947–7966. 10.1021/JACS.5B04641/ASSET/IMAGES/LARGE/JA-2015-04641K_0019.JPEG. [PubMed: 26020837]

(18). Gao J; Bender CM; Murphy CJ Dependence of the Gold Nanorod Aspect Ratio on the Nature of the Directing Surfactant in Aqueous Solution. Langmuir 2003, 19 (21), 9065–9070. 10.1021/LA034919I/ASSET/IMAGES/MEDIUM/LA034919IE00001.GIF.

(19). Safo IA; Werheid M; Dosche C; Oezaslan M The Role of Polyvinylpyrrolidone (PVP) as a Capping and Structure-Directing Agent in the Formation of Pt Nanocubes. Nanoscale Advances 2019, 1 (8), 3095–3106. 10.1039/C9NA00186G. [PubMed: 36133604]

(20). Puntes VF; Zanchet D; Erdonmez CK; Alivisatos AP Synthesis of Hcp-Co Nanodisks. 2002. 10.1021/ja027262g.

(21). Luther JM; Jain PK; Ewers T; Alivisatos AP Localized Surface Plasmon Resonances Arising from Free Carriers in Doped Quantum Dots. Nature Materials 2011 10:5 2011, 10 (5), 361–366. 10.1038/nmat3004.

(22). Caragheorgheopol A; Chechik V Mechanistic Aspects of Ligand Exchange in Au Nanoparticles. Physical Chemistry Chemical Physics 2008, 10 (33), 5029–5041. 10.1039/B805551C. [PubMed: 18701949]

(23). Hostetler MJ; Templeton AC; Murray RW Dynamics of Place-Exchange Reactions on Monolayer-Protected Gold Cluster Molecules. Langmuir 1999, 15 (11), 3782–3789. 10.1021/LA981598F/SUPPL_FILE/LA981598F_S.PDF.

(24). Sperling RA; Parak WJ Surface Modification, Functionalization and Bioconjugation of Colloidal Inorganic Nanoparticles. Philosophical Transactions of the Royal Society A: Mathematical, Physical and Engineering Sciences 2010, 368 (1915), 1333–1383. 10.1098/RSTA.2009.0273.

(25). Ahangaran F; Navarchian AH Recent Advances in Chemical Surface Modification of Metal Oxide Nanoparticles with Silane Coupling Agents: A Review. Advances in Colloid and Interface Science 2020, 286, 102298. 10.1016/J.CIS.2020.102298. [PubMed: 33171357]

(26). Suk JS; Xu Q; Kim N; Hanes J; Ensign LM PEGylation as a Strategy for Improving Nanoparticle-Based Drug and Gene Delivery HHS Public Access Graphical Abstract. Adv Drug Deliv Rev 2016, 99, 28–51. 10.1016/j.addr.2015.09.012. [PubMed: 26456916]

(27). Fernandes R; Smyth NR; Muskens OL; Nitti S; Heuer-Jungemann A; Ardem-Jones MR; Kanaras AG Interactions of Skin with Gold Nanoparticles of Different Surface Charge, Shape, and Functionality. Small 2015, 11 (6), 713–721. 10.1002/SMLL.201401913. [PubMed: 25288531]

(28). Kirtane AR; Kalscheuer SM; Panyam J Exploiting Nanotechnology to Overcome Tumor Drug Resistance: Challenges and Opportunities. Advanced drug delivery reviews 2013, 65 (0), 1731–1747. 10.1016/J.ADDR.2013.09.001. [PubMed: 24036273]

(29). Veiseh O; Gunn JW; Zhang M Design and Fabrication of Magnetic Nanoparticles for Targeted Drug Delivery and Imaging. Advanced Drug Delivery Reviews. Elsevier March 8, 2010, pp 284–304. 10.1016/j.addr.2009.11.002.

(30). Scinto SL; Bilodeau DA; Hincapie R; Lee W; Nguyen SS; Xu M; am Ende CW; Finn MG; Lang K; Lin Q; Pezacki JP; Prescher JA; Robillard MS; Fox JM Bioorthogonal Chemistry. Nature Reviews Methods Primers 2021 1:1 2021, 1 (1), 1–23. 10.1038/s43586-021-00028-z.

(31). Sletten EM; Bertozzi CR From Mechanism to Mouse: A Tale of Two Bioorthogonal Reactions. Accounts of Chemical Research 2011, 44 (9), 666–676. 10.1021/AR200148Z/ASSET/IMAGES/LARGE/AR-2011-00148Z_0014.JPEG. [PubMed: 21838330]

(32). Darko A; Wallace S; Dmitrenko O; Machovina MM; Mehl RA; Chin JW; Fox JM Conformationally Strained Trans-Cyclooctene with Improved Stability and Excellent Reactivity

in Tetrazine Ligation. Chemical Science 2014, 5 (10), 3770–3776. 10.1039/C4SC01348D. [PubMed: 26113970]

(33). Li Y; Yang L Driving Forces for Drug Loading in Drug Carriers. 10.3109/02652048.2015.1010459 2015, 32 (3), 255–272. 10.3109/02652048.2015.1010459.

(34). Yu G; Chen X Host-Guest Chemistry in Supramolecular Theranostics. Theranostics 2019, 9 (11), 3041. 10.7150/THNO.31653. [PubMed: 31244941]

(35). Li X; Takashima M; Yuba E; Harada A; Kono K PEGylated PAMAM Dendrimer–Doxorubicin Conjugate-Hybridized Gold Nanorod for Combined Photothermal-Chemotherapy. Biomaterials 2014, 35 (24), 6576–6584. 10.1016/J.BIOMATERIALS.2014.04.043. [PubMed: 24816361]

(36). Jeon M; Lin G; Stephen ZR; Kato FL; Zhang M Paclitaxel-Loaded Iron Oxide Nanoparticles for Targeted Breast Cancer Therapy. Advanced Therapeutics 2019, 2 (12), 1900081. 10.1002/adtp.201900081.

(37). Mintzer MA; Simanek EE Nonviral Vectors for Gene Delivery. Chemical Reviews. American Chemical Society February 11, 2009, pp 259–302. 10.1021/cr800409e.

(38). Sung YK; Kim SW Recent Advances in Polymeric Drug Delivery Systems. Biomaterials Research 2020 24:1 2020, 24 (1), 1–12. 10.1186/S40824-020-00190-7.

(39). Deng H; Liu J; Zhao X; Zhang Y; Liu J; Xu S; Deng L; Dong A; Zhang J PEG-b-PCL Copolymer Micelles with the Ability of PH-Controlled Negative-to-Positive Charge Reversal for Intracellular Delivery of Doxorubicin. Biomacromolecules 2014, 15 (11), 4281–4292. 10.1021/BM501290T/SUPPL_FILE/BM501290T_SI_001.PDF. [PubMed: 25325531]

(40). Li F; Lu J; Kong X; Hyeon T; Ling D Dynamic Nanoparticle Assemblies for Biomedical Applications. Advanced Materials 2017, 29 (14). 10.1002/ADMA.201605897.

(41). Li F; Du Y; Liu J; Sun H; Wang J; Li R; Kim D; Hyeon T; Ling D; Li F; Du Y; Sun H; Wang J; Li R; Ling D; Liu J; Kim D; Hyeon T Responsive Assembly of Upconversion Nanoparticles for PH-Activated and Near-Infrared-Triggered Photodynamic Therapy of Deep Tumors. Advanced Materials 2018, 30 (35), 1802808. 10.1002/ADMA.201802808.

(42). Li F; Liang Z; Liu J; Sun J; Hu X; Zhao M; Liu J; Bai R; Kim D; Sun X; Hyeon T; Ling D Dynamically Reversible Iron Oxide Nanoparticle Assemblies for Targeted Amplification of T1-Weighted Magnetic Resonance Imaging of Tumors. Nano Letters 2019, 19 (7), 4213–4220. 10.1021/ACS.NANOLETT.8B04411/ASSET/IMAGES/LARGE/NL-2018-04411P_0004.JPEG. [PubMed: 30719918]

(43). Prabhakar U; Maeda H; Jain RK; Sevick-Muraca EM; Zamboni W; Farokhzad OC; Barry ST; Gabizon A; Grodzinski P; Blakey DC Challenges and Key Considerations of the Enhanced Permeability and Retention Effect for Nanomedicine Drug Delivery in Oncology. Cancer Research 2013, 73 (8), 2412–2417. 10.1158/0008-5472.CAN-12-4561/651197/AM/CHALLENGES-AND-KEY-CONSIDERATIONS-OF-THE-ENHANCED. [PubMed: 23423979]

(44). Pandit S; Dutta D; Nie S Active Transcytosis and New Opportunities for Cancer Nanomedicine. Nature Materials 2020 19:5 2020, 19 (5), 478–480. 10.1038/s41563-020-0672-1.

(45). Zhang Y; He J Tumor Vasculature-Targeting Nanomedicines. Acta Biomaterialia 2021, 134, 1–12. 10.1016/J.ACTBIO.2021.07.015. [PubMed: 34271167]

(46). Ju X; Chen H; Miao T; Ni J; Han L Prodrug Delivery Using Dual-Targeting Nanoparticles to Treat Breast Cancer Brain Metastases. Molecular Pharmaceutics 2021, 18 (7), 2694–2702. 10.1021/ACS.MOLPHARMACEUT.1C00224/ASSET/IMAGES/LARGE/MP1C00224_0006.JPEG. [PubMed: 34109794]

(47). Suzuki K; Miura Y; Mochida Y; Miyazaki T; Toh K; Anraku Y; Melo V; Liu X; Ishii T; Nagano O; Saya H; Cabral H; Kataoka K Glucose Transporter 1-Mediated Vascular Translocation of Nanomedicines Enhances Accumulation and Efficacy in Solid Tumors. Journal of Controlled Release 2019, 301, 28–41. 10.1016/J.JCONREL.2019.02.021. [PubMed: 30844476]

(48). Liu R; Fu Z; Zhao M; Gao X; Li H; Mi Q; Liu P; Yang J; Yao Z; Gao Q GLUT1-Mediated Selective Tumor Targeting with Fluorine Containing Platinum(II) Glycoconjugates. Oncotarget 2017, 8 (24), 39476. 10.18632/ONCOTARGET.17073. [PubMed: 28467806]

(49). Sweeney MD; Sagare AP; Zlokovic BV Blood–Brain Barrier Breakdown in Alzheimer Disease and Other Neurodegenerative Disorders. Nature Reviews Neurology 2018 14:3 2018, 14 (3), 133–150. 10.1038/nrneurol.2017.188.

(50). Anraku Y; Kuwahara H; Fukusato Y; Mizoguchi A; Ishii T; Nitta K; Matsumoto Y; Toh K; Miyata K; Uchida S; Nishina K; Osada K; Itaka K; Nishiyama N; Mizusawa H; Yamasoba T; Yokota T; Kataoka K Glycaemic Control Boosts Glucosylated Nanocarrier Crossing the BBB into the Brain. Nature Communications 2017 8:1 2017, 8 (1), 1–9. 10.1038/s41467-017-00952-3.

(51). Stephen ZR; Kievit FM; Veiseh O; Chiarelli PA; Fang C; Wang K; Hatzinger SJ; Ellenbogen RG; Silber JR; Zhang M Redox-Responsive Magnetic Nanoparticle for Targeted Convection-Enhanced Delivery of O 6-Benzylguanine to Brain Tumors. 2014. 10.1021/nn503735w.

(52). Alkilany AM; Zhu L; Weller H; Mews A; Parak WJ; Barz M; Feliu N Ligand Density on Nanoparticles: A Parameter with Critical Impact on Nanomedicine. Advanced Drug Delivery Reviews. Elsevier B.V. March 15, 2019, pp 22–36. 10.1016/j.addr.2019.05.010.

(53). Mi P; Cabral H; Kataoka K; Mi P; Cabral H; Kataoka K Ligand-Installed Nanocarriers toward Precision Therapy. Advanced Materials 2020, 32 (13), 1902604. 10.1002/ADMA.201902604.

(54). Liang D; Dahal U; Wu M; Murphy CJ; Cui Q Ligand Length and Surface Curvature Modulate Nanoparticle Surface Heterogeneity and Electrostatics. Journal of Physical Chemistry C 2020, 124 (44), 24513–24525. 10.1021/ACS.JPCC.0C08387/ASSET/IMAGES/LARGE/JP0C08387_0009.JPEG.

(55). Li X; Coulter Montague E; Pollinzi A; Lofts A; Hoare T; Li X; Montague EC; Pollinzi A; Hoare T; Lofts A Design of Smart Size-, Surface-, and Shape-Switching Nanoparticles to Improve Therapeutic Efficacy. Small 2022, 18 (6), 2104632. 10.1002/SMLL.202104632.

(56). Kwon EJ; Dudani JS; Bhatia SN Ultrasensitive Tumour-Penetrating Nanosensors of Protease Activity. Nature Biomedical Engineering 20171:4 2017, 1 (4), 1–10. 10.1038/s41551-017-0054.

(57). Li D; Ma Y; Du J; Tao W; Du X; Yang X; Wang J Tumor Acidity/NIR Controlled Interaction of Transformable Nanoparticle with Biological Systems for Cancer Therapy. Nano Letters 2017, 17 (5), 2871–2878. 10.1021/ACS.NANOLETT.6B05396/ASSET/IMAGES/LARGE/NL-2016-05396K_0005.JPEG. [PubMed: 28375632]

(58). Lee ES; Gao Z; Kim D; Park K; Kwon IC; Bae YH Super PH-Sensitive Multifunctional Polymeric Micelle for Tumor PHe Specific TAT Exposure and Multidrug Resistance. Journal of Controlled Release 2008, 129 (3), 228–236. 10.1016/J.JCONREL.2008.04.024. [PubMed: 18539355]

(59). Ding Y; Liu J; Zhang Y; Li X; Ou H; Cheng T; Ma L; An Y; Liu J; Huang F; Liu Y; Shi L A Novel Strategy Based on a Ligand-Switchable Nanoparticle Delivery System for Deep Tumor Penetration. Nanoscale Horizons 2019, 4 (3), 658–666. 10.1039/C8NH00415C.

(60). Xu W; Qian J; Hou G; Wang Y; Wang J; Sun T; Ji L; Suo A; Yao Y A Dual-Targeted Hyaluronic Acid-Gold Nanorod Platform with Triple-Stimuli Responsiveness for Photodynamic/Photothermal Therapy of Breast Cancer. Acta Biomaterialia 2019, 83, 400–413. 10.1016/J.ACTBIO.2018.11.026. [PubMed: 30465921]

(61). Wilhelm S; Tavares AJ; Dai Q; Ohta S; Audet J; Dvorak HF; Chan WCW Analysis of Nanoparticle Delivery to Tumours. Nature Review s Materials 2016 1:5 2016, 1 (5), 1–12. 10.1038/natrevmats.2016.14.

(62). Dai Q; Wilhelm S; Ding D; Syed AM; Sindhwani S; Zhang Y; Chen YY; Macmillan P; Chan WCW Quantifying the Ligand-Coated Nanoparticle Delivery to Cancer Cells in Solid Tumors. ACS Nano 2018, 12 (8), 8423–8435. 10.1021/ACSNANO.8B03900/SUPPL_FILE/NN8B03900_SI_001.PDF. [PubMed: 30016073]

(63). He Z; Zhang Y; Feng N Cell Membrane-Coated Nanosized Active Targeted Drug Delivery Systems Homing to Tumor Cells: A Review. Materials Science and Engineering: C 2020, 106, 110298. 10.1016/J.MSEC.2019.110298. [PubMed: 31753336]

(64). Li R; He Y; Zhang S; Qin J; Wang J Cell Membrane-Based Nanoparticles: A New Biomimetic Platform for Tumor Diagnosis and Treatment. Acta Pharmaceutica Sinica B 2018, 8 (1), 14–22. 10.1016/J.APSB.2017.11.009. [PubMed: 29872619]

(65). Mitchell MJ; Billingsley MM; Haley RM; Wechsler ME; Peppas NA; Langer R Engineering Precision Nanoparticles for Drug Delivery. Nature Reviews Drug Discovery 2020 20:2 2020, 20 (2), 101–124. 10.1038/s41573-020-0090-8.

(66). Reguera J; Jiménez De Aberasturi D; Henriksen-Lacey M; Langer J; Espinosa A; Szczupak B; Wilhelm C; Liz-Marzán LM Janus Plasmonic–Magnetic Gold–Iron Oxide Nanoparticles

as Contrast Agents for Multimodal Imaging. Nanoscale 2017, 9 (27), 9467–9480. 10.1039/C7NR01406F. [PubMed: 28660946]

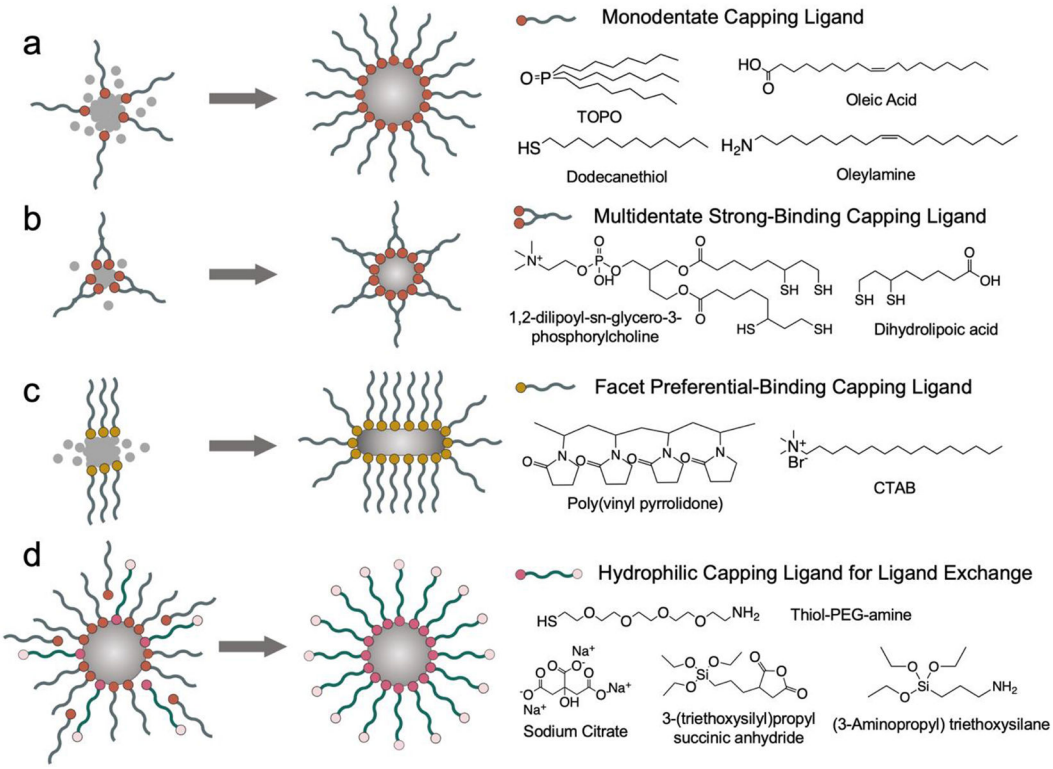

Figure 1.

Capping ligands' influences on inorganic nanoparticle core. (a) A monodentate capping ligand stabilizes core growth. (b) A strong-binding multidentate ligand facilitates the formation of smaller cores. (c) A capping ligand with preferential facet binding results in anisotropic growth. (d) Ligand exchange renders core's surface hydrophilic.

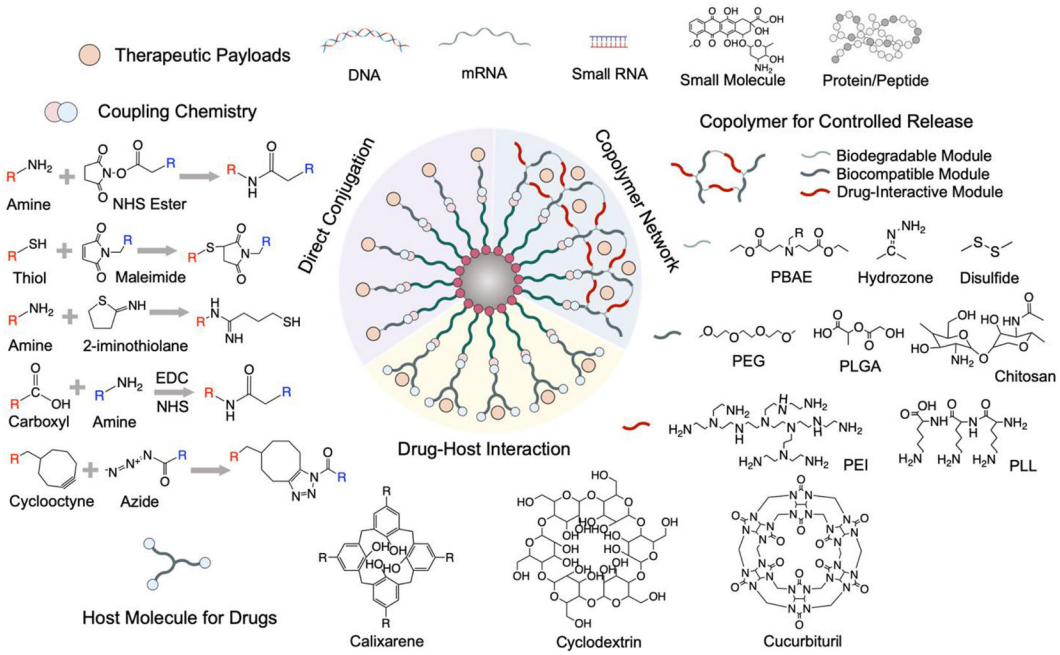

Figure 2.

Overview of representative nanoparticle drug loading moieties and their coupling chemistry.

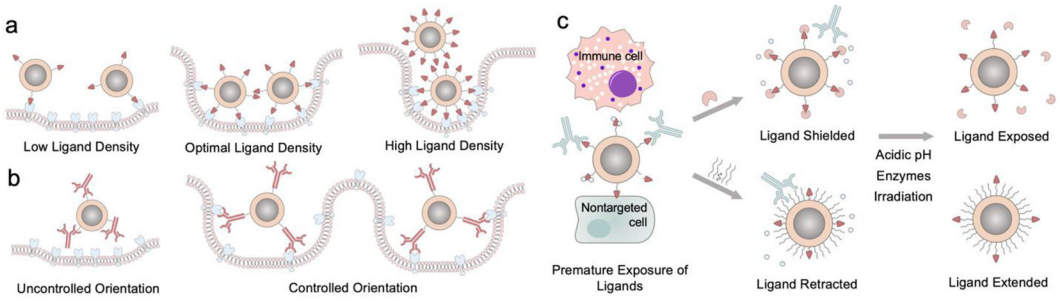

Figure 3.

Critical factors of installation of targeting ligands on nanoparticles. (a) The density of targeting ligand determines nanoparticle's cell uptake efficiency. (b) The orientation of large targeting ligands needs to be controlled for optimal cell entry. (c) Ligand protection moieties for preventing premature exposure of ligands.

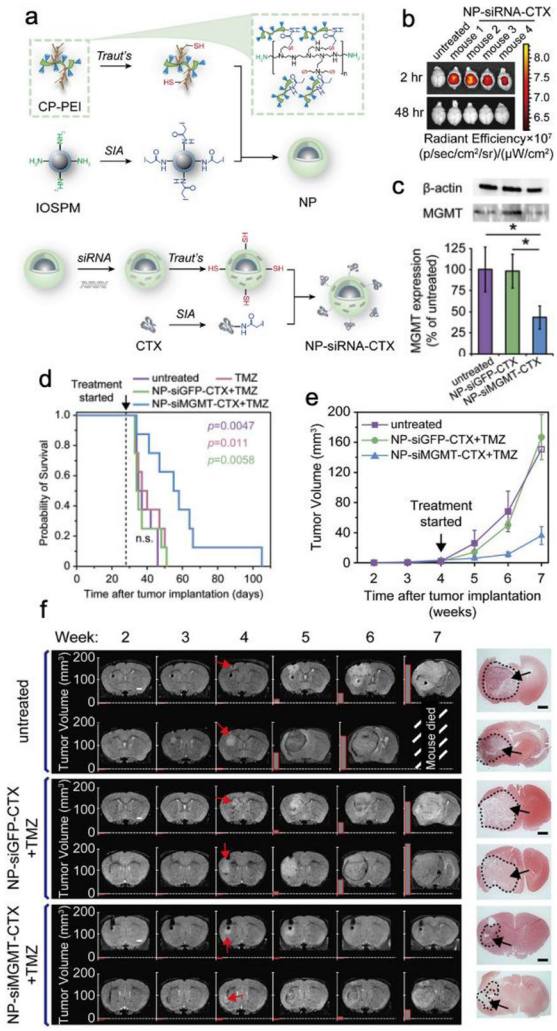

Figure 4.

BBB-targeted nanoparticle-mediated delivery of siRNA for chemotherapeutic sensitization. (a) Schematic illustration of NP–siRNA–CTX synthesis process. (b) Fluorescence images of NP–siRNA–CTX (red)'s mouse brains accumulation. (c) The expression of MGMT and β-actin protein in tumor sections harvested from the treated GBM6-bearing mice. (d) Kaplan–Meier survival curves of mice receiving different treatments. (e) Tumor volume measurements for mice receiving different treatments. (f) MRI images of representative mouse brains. Red arrows mark the onset of tumor. The last column on the right shows H&E-stained whole brain section images. Adapted with permission from ref 1, copyright 2020, John Wiley and Sons.

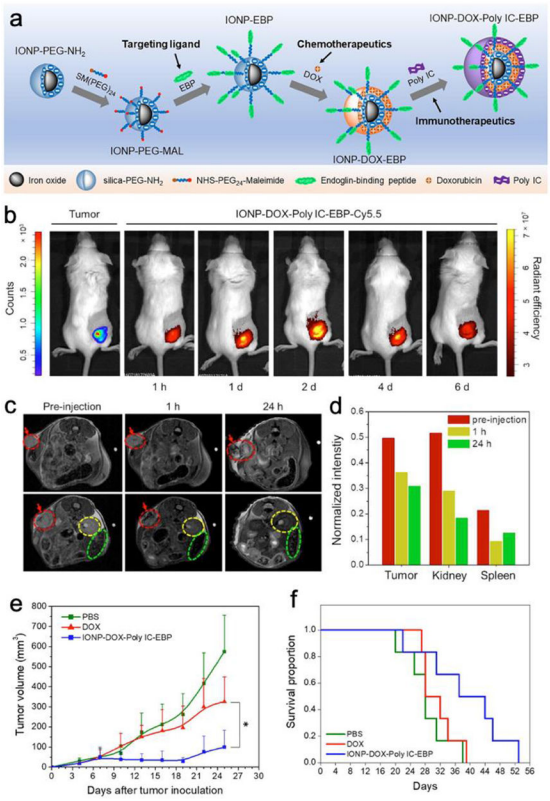

Figure 5.

Iron oxide nanoparticles co-deliver chemo and immunotherapeutic drugs for TNBC treatment. (a) Schematic illustration of the synthesis of IONP-DOX-Poly IC-EBP. (b) Fluorescence images of mice bearing 4T1-luc tumors and treated with IONP–DOX–Poly IC–EBP–Cy5.5. (c) MR imaging of mice bearing 4T1 tumors treated by IONP–DOX–Poly IC–EBP–Cy5.5. Tumors are indicated by red arrows and dashed circles; kidney and spleen are indicated by yellow and green dashed circles, respectively. (d) Quantitation of the relative MR intensity in (e). (f and f) Tumor size measurement and Kaplan–Meier survival curves of the treated mice. Adapted with permission from ref 2, copyright 2021, Elsevier.

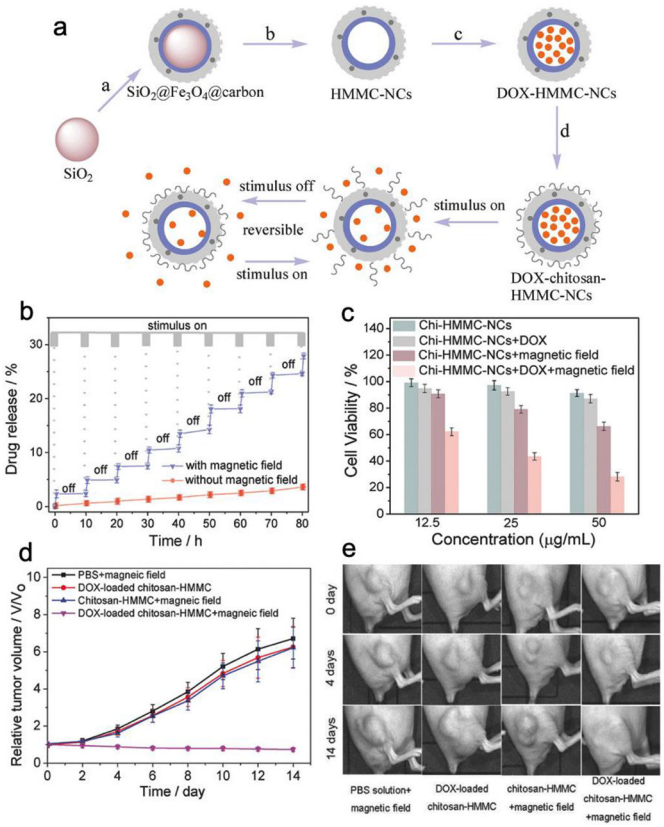

Figure 6.

Switchable double-gated chemotherapeutic drug release for breast cancer treatment. (a) Schematic design of chitosan-HMMC-NC nanoparticle. a) Surface coating of SiO2 core. b) Erosion of the SiO2 core to form HMMC-NCs. c) Loading of DOX into HMMC-NCs. d) Surface modification of DOX-HMMC-NCs with chitosan. (b) DOX release profile of chitosan-HMMC-NCs. (c) In vitro cytotoxicity profiles. (d) The tumor volume growth curves of mice receiving various treatments. (e) Photographs of mice's tumors under various treatments. Adapted with permission from ref 3, copyright 2017, John Wiley and Sons.

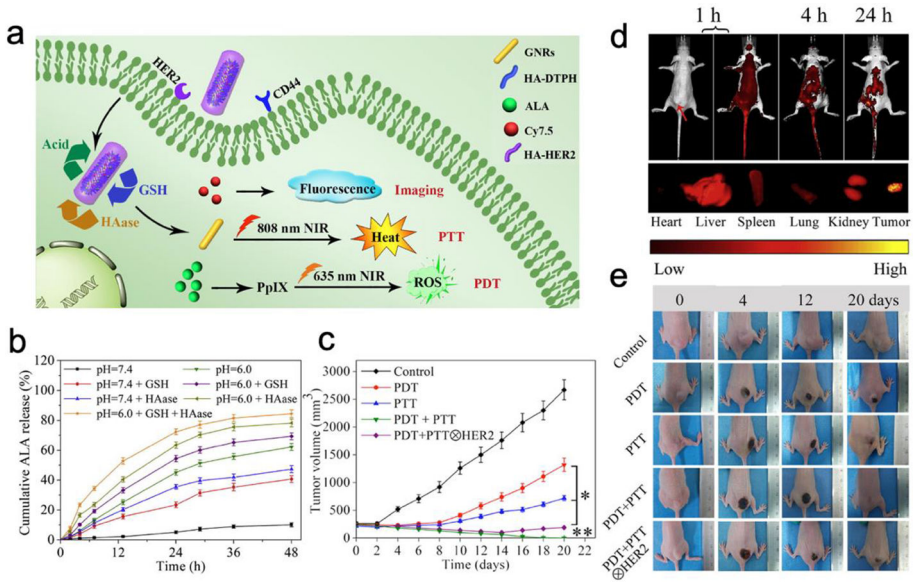

Figure 7.

Gold nanorod equipped with dual targeting ligands for photothermal-photodynamic combination therapy against breast tumors. (a) Schematic representation of GNR-HA–ALA/Cy7.5-HER2. (b) ALA release profiles from GNR-HA–ALA/Cy7.5-HER2. (c) In vivo fluorescence imaging of a representative tumor-bearing mouse treated with GNR-HA–ALA/Cy7.5-HER2 (top); ex vivo imaging of tumor and major organs (bottom). Red arrow indicates the tumor. (d) Tumor volume measurement of mice receiving various treatments. (e) Representative photos of mice bearing tumors at different treatment stages. Adapted with permission from ref 60, copyright 2019, Elsevier.